(NASA-CR-168610) MANUFACTURING IN SPACE: FLUID DYNAMICS NUMERICAL ANALYSIS Annual Report, Aug. 1980 - Aug. 1981 (Lockheed Missiles and Space Co.) 51 p HC A04/MF A01 CSCL 22A G3/12

N82-19236

Unclas 15118

MANUFACTURING IN SPACE: FLUID DYNAMICS NUMERICAL ANALYSIS

August 1981

Contract NASW-3281 (Annual Report)

Prepared for

NASA HEADQUARTERS
WASHINGTON, DC 20546

by

S. J. Robertson
L. A. Nicholson
L. W. Spradley

Lockheed Missiles & Space Company, Inc.
Huntsville Research & Engineering Center
4800 Bradford Drive, Huntsville, AL 35807

FOREWORD

This document is an annual report describing the results of effort by personnel of Lockheed Missiles & Space Company, Inc., Huntsville Research & Engineering Center, for the National Aeronautics and Space Administration under Contract NASW-3281, "Manufacturing in Space: Fluid Dynamics Numerical Analysis." The contractual effort described in this document was performed during the year from August 1980 to August 1981. The NASA Technical Director for this contract is Dr. Robert F. Dressler, Manager, Advanced Technology Program, NASA Headquarters, Washington, DC.

ACKNOWLEDGMENT

The authors are pleased to acknowledge the contribution to this effort of the NASA Technical Director, Dr. Robert F. Dressler. His suggestions and guidance contributed substantially to the overall program.

CONTENTS

	Page
FOREWORD	ii
ACKNOWLEDGMENT	ii
INTRODUCTION	1
PART 1: NUMERICAL SIMULATION OF NATURAL CONVECTION IN A SPHERICAL CONTAINER DUE TO COOLING AT THE CENTER (IDEALIZATION OF THE LAL/KROES EXPERIMENT).	
PART 2: NUMERICAL SIMULATION OF NATURAL CONVECTION WITH GRAVITY-SHIFT IN CIRCULAR CYLINDERS IN LOW GRAVITY	
PART 3: EFFECT OF CONTAINER SHAPE ON NATURAL CONVECTION IN ENCLOSURES.	

INTRODUCTION

There is considerable current interest in the possibility of utilizing the near-zero gravity environment aboard orbiting space stations for various materials processing applications. There are a number of potential applications where the near absence of convective stirring during the process would presumably enhance the quality of the product. The purpose of the research program described in this document is to perform numerical computations of thermally induced convection for various experiment configurations under microgravity conditions simulating the orbiting space station environment. The research program was initiated in August 1979. This document is an annual report summarizing the results of effort during the year from August 1980 to August 1981.

Three basic tasks were performed during this year's effort:

1. An analysis was performed of thermal convection in the Lal/Kroes experiment configuration. The analysis was based on a simplified geometry where three-dimensional flow conditions in the cubical shaped container were approximated by axisymmetric flow in a spherical shaped container of equal volume.
2. An analysis was performed of thermal convection in a two-dimensional circular enclosure where the gravity vector changes in both magnitude and direction.
3. An analysis was performed of the effect of container shape on the intensity of natural convection. Results were obtained for two-dimensional enclosures of circular, half-circular and square shaped cross sections.

The results of these tasks are described in the following Parts 1, 2 and 3 of this document.

Part 1

NUMERICAL SIMULATION OF NATURAL CONVECTION IN A SPHERICAL CONTAINER DUE TO COOLING AT THE CENTER (IDEALIZATION OF THE LAL/KROES EXPERIMENT)

ABSTRACT

Natural convection in a spherical container with cooling at the center was numerically simulated using the Lockheed-developed General Interpolants Method (GIM) numerical fluid dynamics computer program. The numerical analysis was simplified by assuming axisymmetric flow in the spherical container, with the symmetry axis being a sphere diagonal parallel to the gravity vector. This axisymmetric spherical geometry was intended as an idealization of the proposed Lal/Kroes crystal growing experiment to be performed on board Spacelab. Results were obtained for a range of Rayleigh numbers from 25 to 10,000. For a temperature difference of 10 C from the cooling sting at the center to the container surface, and a gravitational loading of 10^{-6} g_e, a computed maximum fluid velocity of about 2.4×10^{-5} cm/sec was reached after about 250 sec. The computed velocities were found to be approximately proportional to the Rayleigh number over the range of Rayleigh numbers investigated.

CONTENTS

	Page
FOREWORD	ii
ABSTRACT	iii
NOMENCLATURE	v
INTRODUCTION	1
NUMERICAL SIMULATION	2
RESULTS	5
CONCLUSIONS	14
REFERENCE	15

NOMENCLATURE

Symbol	Description
g	gravity force in units of acceleration
g_e	gravitational acceleration on surface of earth, 980 cm/sec^2
r	radial distance
R	sphere radius
Ra	Rayleigh number = $\frac{g\beta \Delta T R^3}{\nu\alpha}$
T	temperature
ΔT	temperature difference between cooled crystal growing surface at center of container and container wall
t	time
$\tilde{t}$	dimensionless time = $\nu t/R^2$
v	velocity
$\tilde{v}$	dimensionless velocity = $\frac{\nu}{g\beta \Delta T R^2} v$
α	thermal diffusivity
β	volumetric coefficient of thermal expansion
ν	kinematic viscosity
ψ	stream function

INTRODUCTION

One of the proposed experiments to be performed using the Fluids Experiment System (FES) facility aboard Spacelab is the Lal/Kroes experiment (Ref. 1), which is concerned with the controlled growth of a single crystal under near-zero gravity conditions. The crystal is to be grown from a triglycine sulfate (TGS) solution contained in a 10 x 10 x 10 cm cubical shaped container. The concentration is to be nominally 45 g TGS/100 cc water. The temperature of the solution will be within the range of 35 to 50 C. The crystal will be grown on a cooled 1 cm diameter disk positioned at the center of the container at the end of a 2 cm diameter insulated sting. The disk will be cooled up to 10 C less than the surrounding container walls.

The purpose of the experiment is to study crystal growth in the absence of significant gravity induced convective stirring of the solution. The near elimination of convective stirring is expected to result in the growth of high quality crystals. The purpose of this numerical study is to predict the intensity of convective stirring due to the small residual gravity forces remaining under orbital flight conditions. The Lockheed developed General Interpolant Method (GIM) code computer program (Ref. 2) was used in the numerical simulations. This computer code numerically integrates the basic fluid dynamics equations in conservation form. Computations were performed on the NASA-Langley Cyber 203.

NUMERICAL SIMULATION

To permit reasonable economy in computer usage, the cubical shaped experiment configuration was modeled by a sphere of the same volume as the cubical container, with axisymmetric flow assumed. The axis of symmetry is along a sphere diameter parallel to the gravity vector. The nodal point distribution was generated by the GIM code geometry module by specifying an array of 20 x 10 area elements and 21 x 11 nodal points over the half-sphere cross section enclosed by a semicircular arc and sphere axis of symmetry. The geometry module treated the semicircular region as a four-sided figure, with the bottom side the axis of symmetry and the other three sides concentric circular arcs. The region was divided into an array of quadrilateral elements with curvilinear sides, and with the nodal points located at the corners of the individual elements. The geometry is shown in Fig. 1 with the computational grid network superimposed. The cooled crystal growing surface is represented by the outline of grid lines at the center of the sphere. The gravity vector is directed downward as shown in the figure.

A steady state conduction temperature distribution is generated by the computer program as an initial condition. The nodal points outlining the cooled crystal growing surface are maintained at a temperature 10 C less than the surrounding container surface.

The physical properties of the TGS solution were not well known at the time of this analysis. Based on conversations with Dr. R. L. Kroes, the NASA Principal Investigator, physical property values were assumed as listed in Table 1.

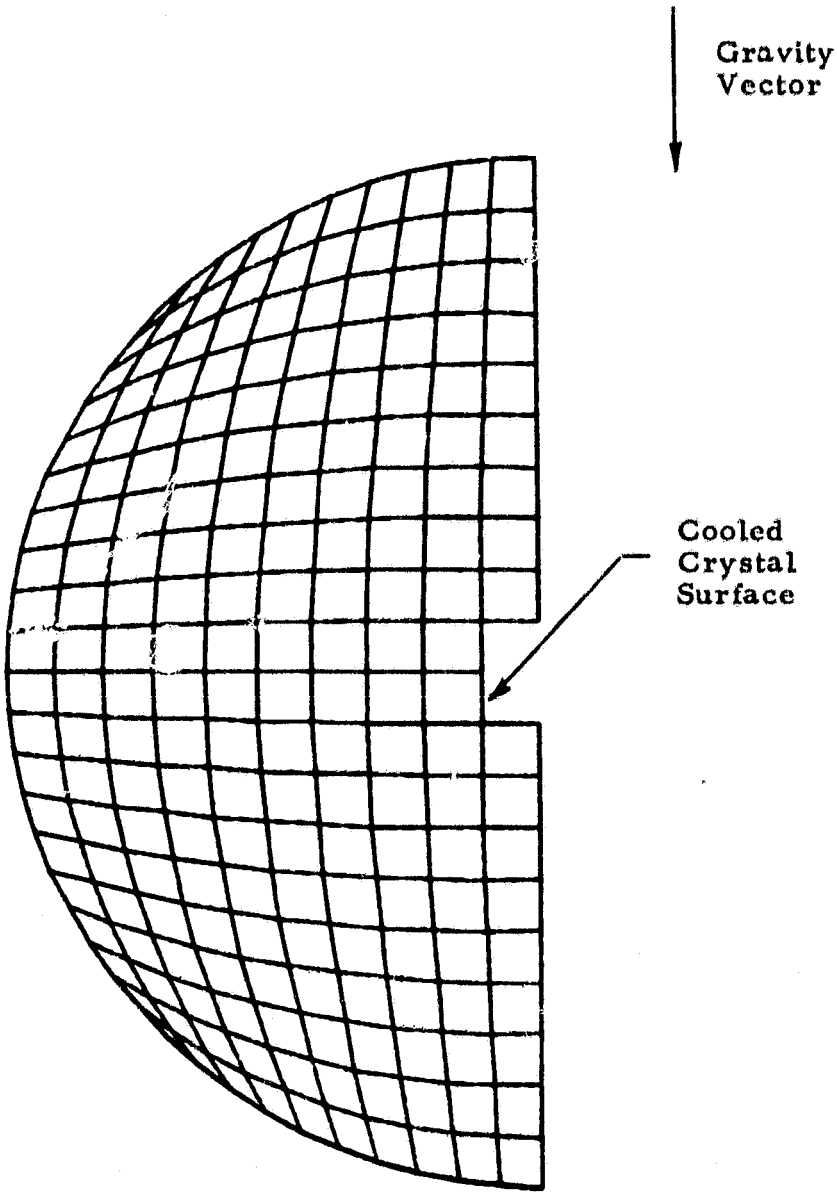

Fig. 1 - Geometry and Computational Grid for Lal/Kroes Experiment Numerical Simulation

Table 1

LIST OF ASSUMED PHYSICAL PROPERTY VALUES FOR TRIGLYCINE SULPHATE (TGS) SOLUTION (45 g TGS/100 cc WATER)

Viscosity, μ	1.78 centipoise
Thermal Conductivity, k	0.00143 cal/cm-sec-C
Density, ρ	1.15 g/cm^3
Specific Heat, C_p	1.0 cal/gm-C
Thermal Expansion Coefficient, β	2.07×10^{-4}/C

RESULTS

Numerical simulations were performed for Rayleigh numbers, Ra, varying from 25 up to 10,000. The computed spatial maximum velocities are plotted in Fig. 2 as a function of time for the various Rayleigh numbers. Note that by nondimensionalizing the velocity and time as shown, the results collapse very closely about a single curve for Rayleigh numbers through 2500. The Ra = 10,000 results are in accord with the other Rayleigh number results through the initial transient up to a dimensionless time of about 0.1.

For the lower Rayleigh numbers, the results shown in Fig. 2 indicate the following approximate relationship for the spatial maximum velocity as a function of time.

$$v_{max} = 0.00485 \frac{g\beta \Delta T R^2}{\nu} \left[1 - \exp\left(-42 \frac{\nu t}{R^2}\right)\right]$$

$$\leq 0.00485 \frac{\alpha}{R} Ra \left[1 - \exp\left(-42 \frac{\nu t}{R^2}\right)\right]$$

For the Lal/Kroes experiment configuration, the equal volume sphere radius, R, corresponding to the 10 x 10 x 10 cm cube is 6.2 cm. The time required to reach steady state is about 250 sec after imposition of an impulse gravitational load. The maximum spatial velocity at steady state is 2.4×10^{-5} cm/sec for a 10^{-6} g_e gravitational load and a 10 C ΔT.

The temperature, streamline and velocity contours at steady state are shown in Figs. 3 through 5 for various Rayleigh numbers. Note that the temperature contour distortion from the conduction profile increases with Rayleigh number as expected. The higher Rayleigh number temperature contours show a strong distortion from the low Rayleigh number results. The streamline contours, however, are basically unchanged over the range of Rayleigh numbers, except for a relatively slight asymmetry introduced at the higher Rayleigh numbers. The flow pattern consists of a single convection cell for all of the Rayleigh numbers shown.

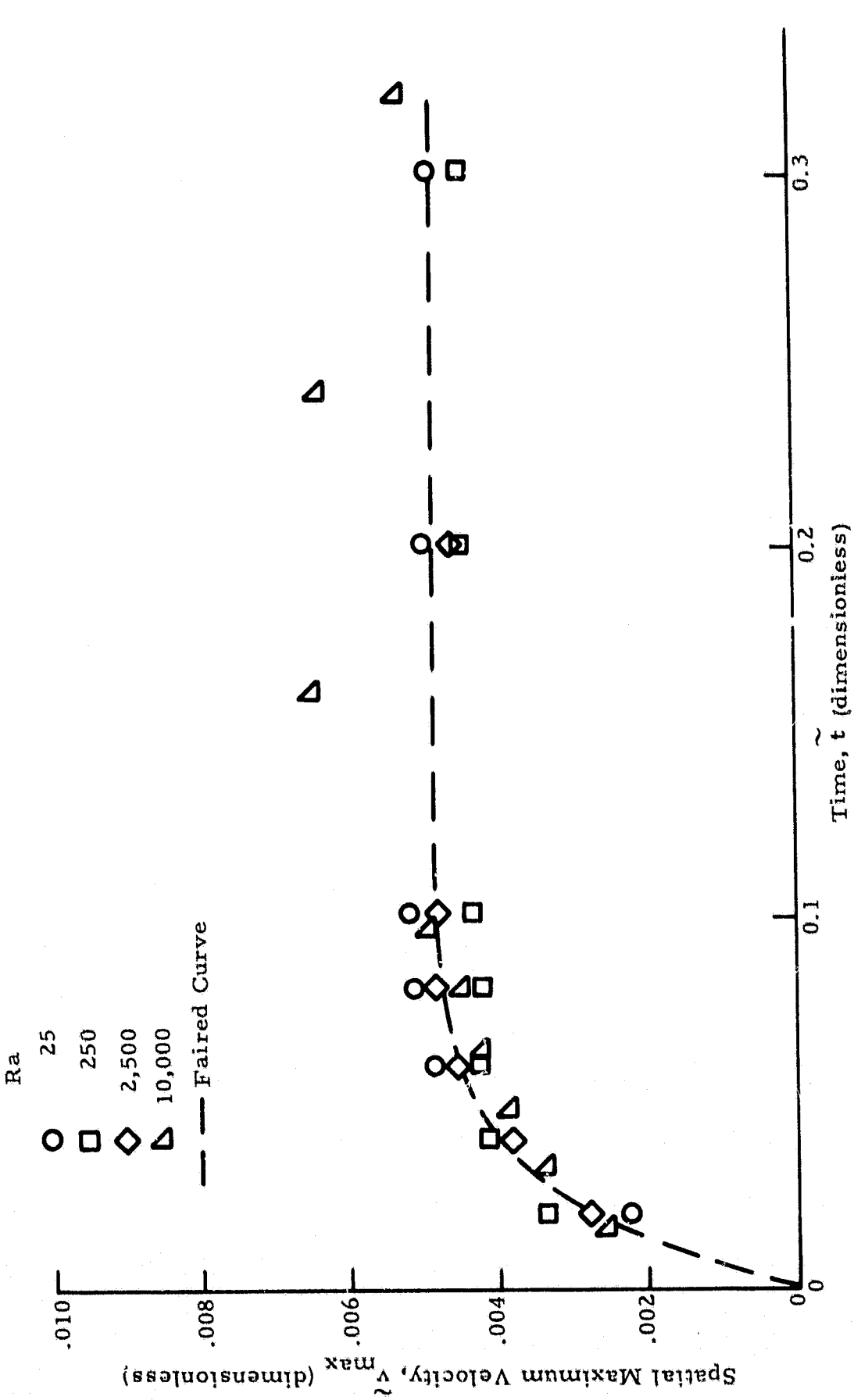

Fig. 2 - Computed Spatial Maximum Velocity History for Idealized Lal/Kroes Experiment for Various Rayleigh Numbers

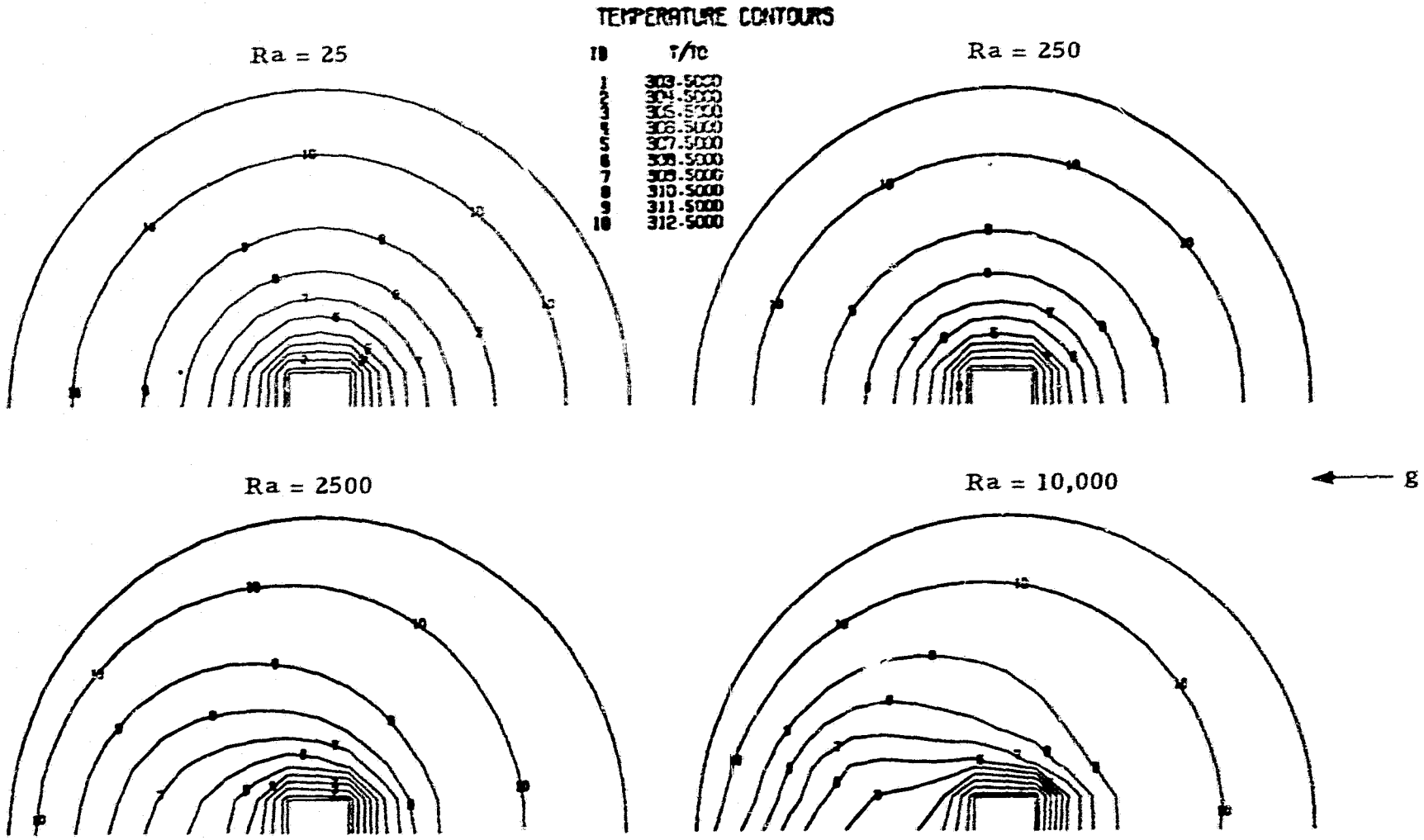

Fig. 3 - Temperature Contours at Steady State for Various Rayleigh Numbers

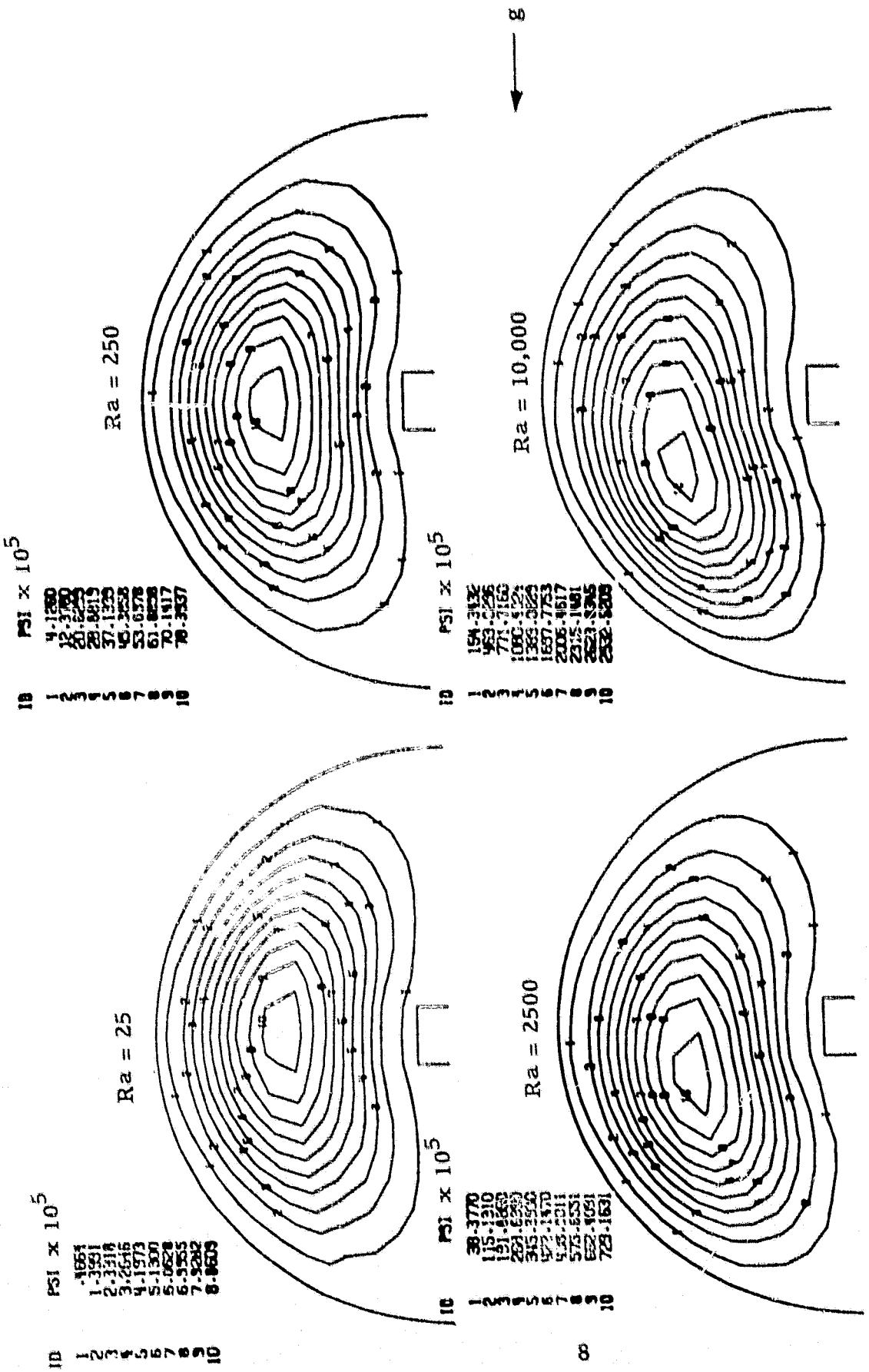

Fig. 4 - Streamline Contours at Steady State for Various Rayleigh Numbers

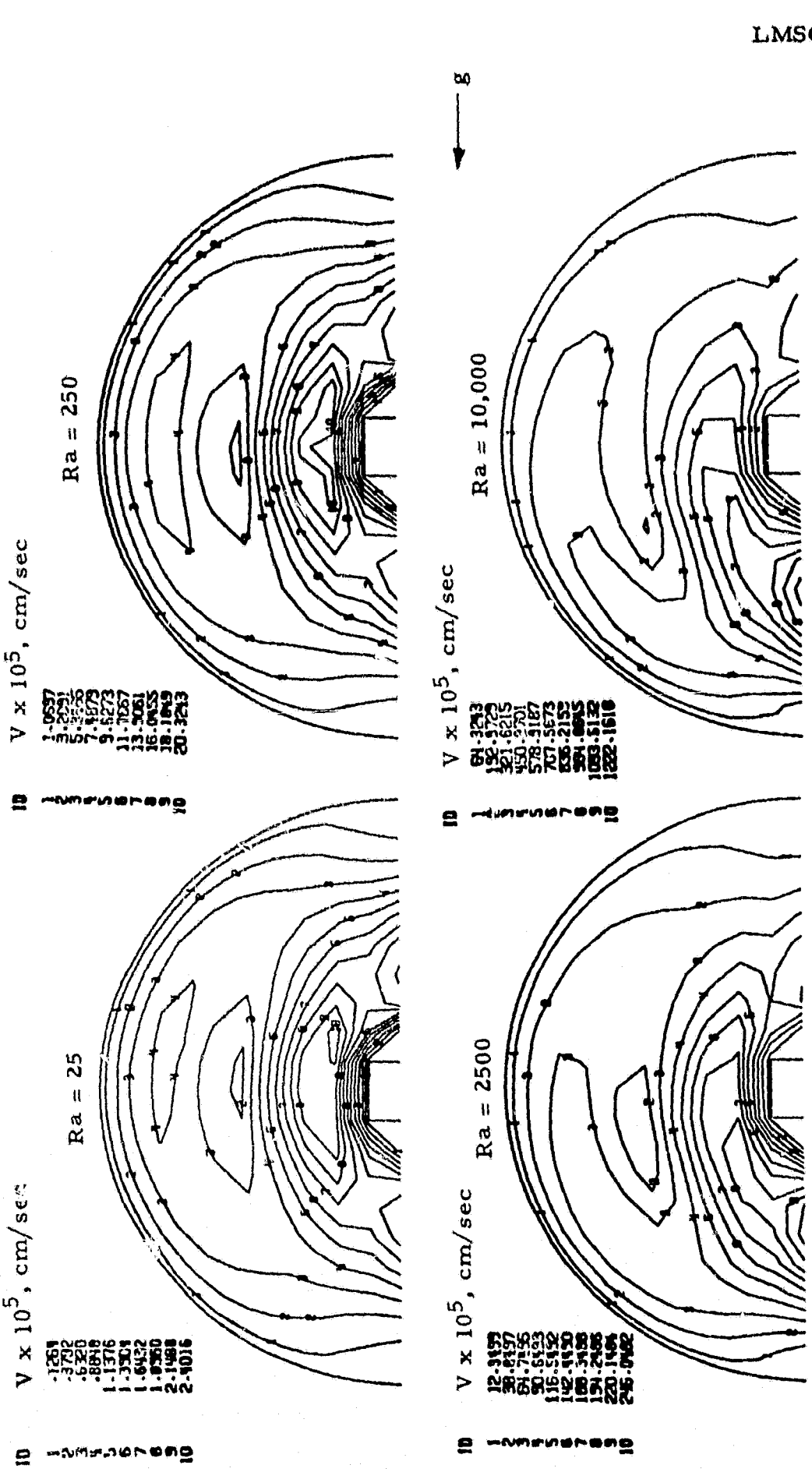

Fig. 5 - Velocity Contours at Steady State for Various Rayleigh Numbers

The variations in temperature, streamline and velocity contours with time are shown in Figs. 6, 7 and 8 for Ra = 10,000. As expected, the distortion in the temperature field increases with time toward the steady state condition. The single convection cell is also shown to shift gradually from the symmetry characteristic of low Rayleigh numbers toward the asymmetry characteristic of high Rayleigh numbers.

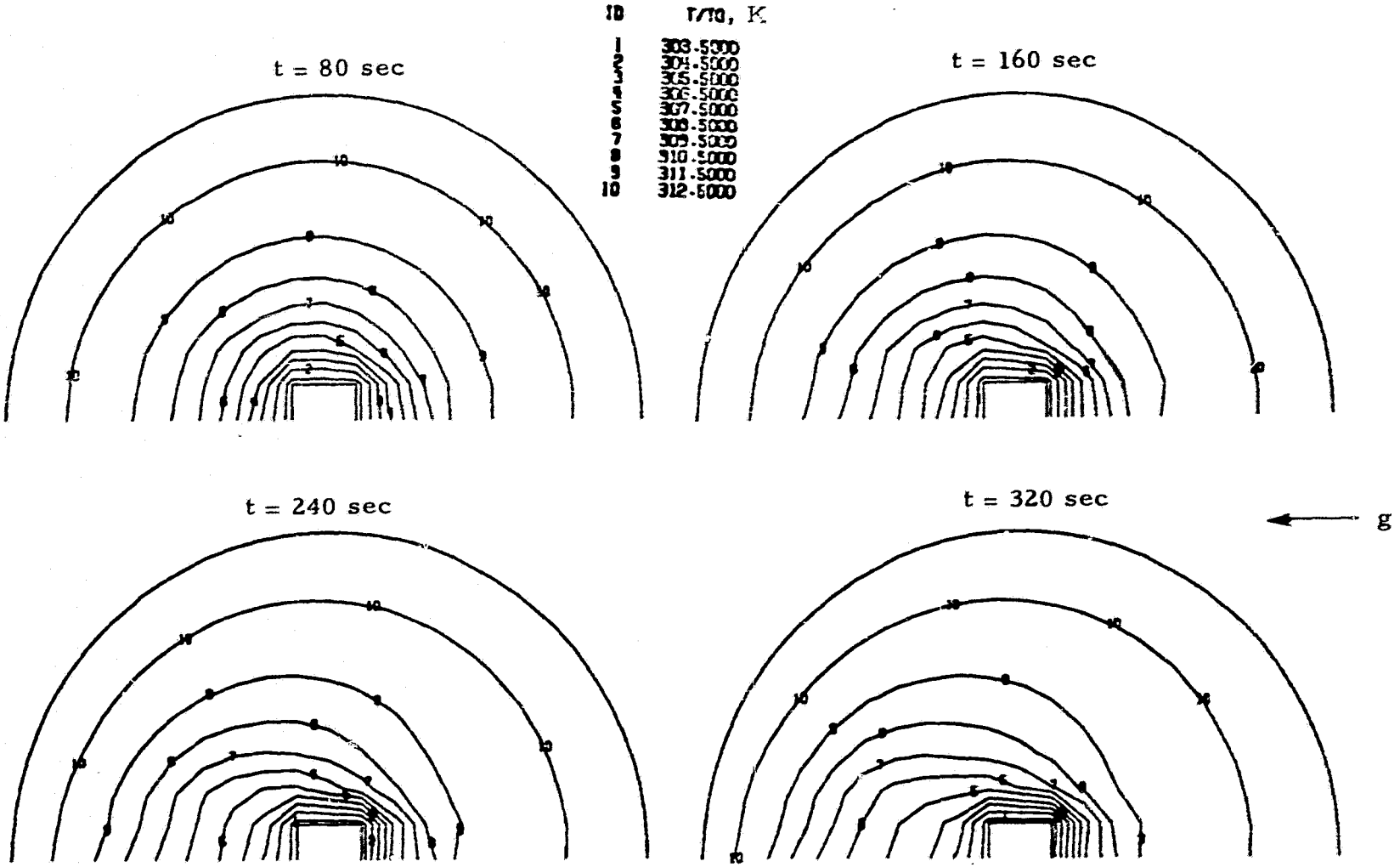

Fig. 6 - Temperature Contours at Various Times for Ra = 10,000

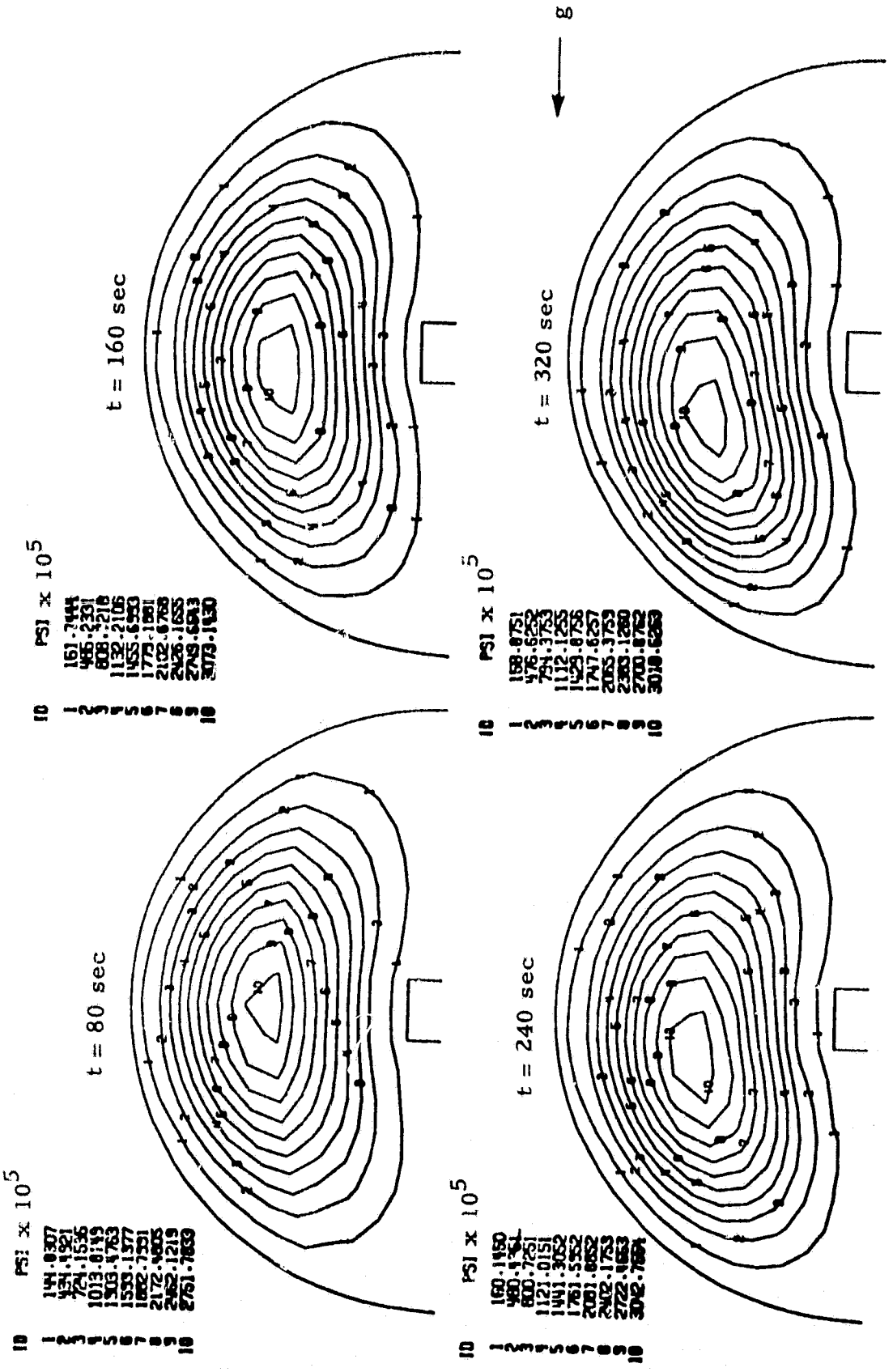

Fig. 7 - Streamline Contours at Various Times for Ra = 10,000

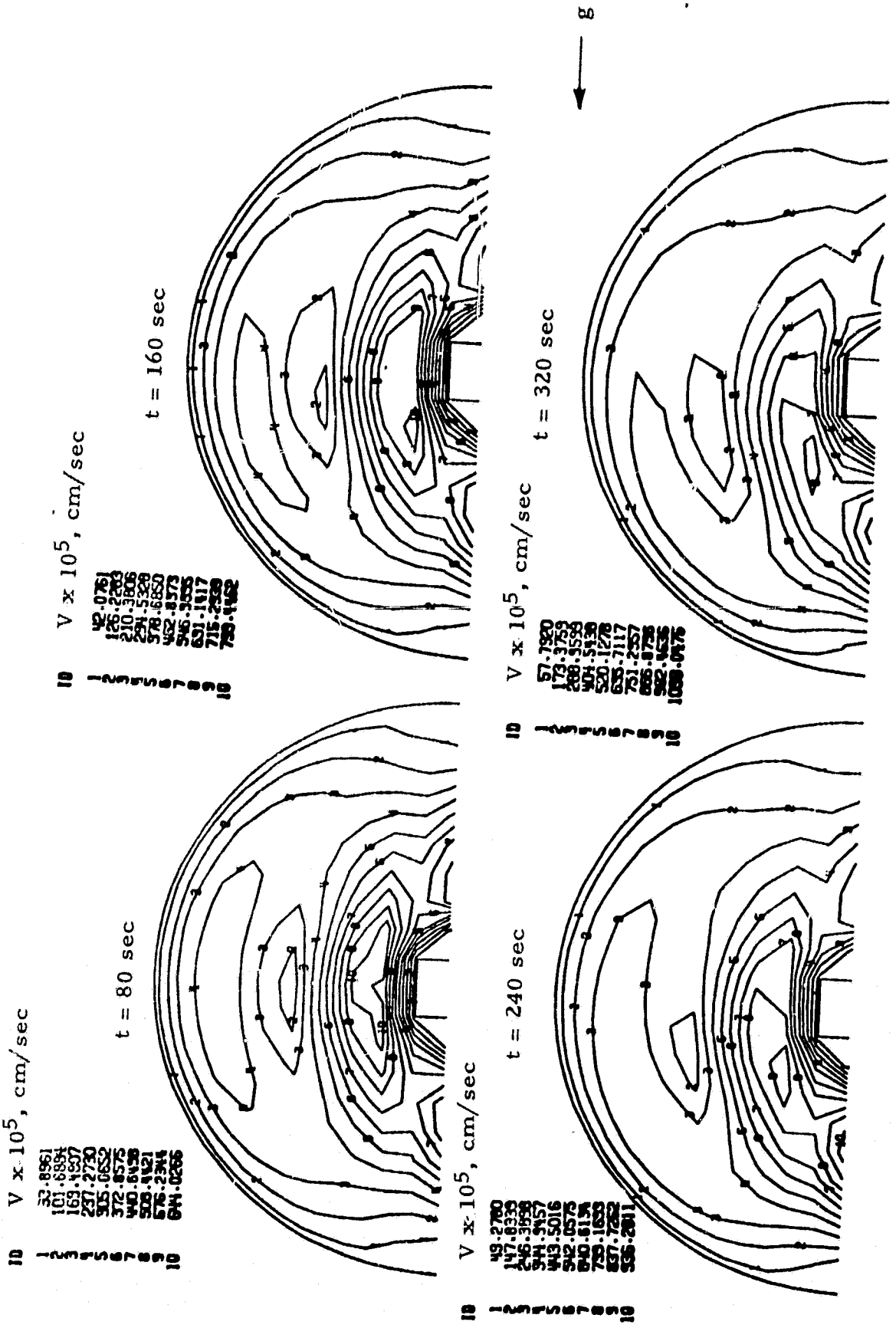

Fig. 8 - Velocity Contours at Various Times for Ra = 10,000

CONCLUSIONS

There are a number of mechanisms other than gravity-induced convection affecting the quality of crystal growth. The results obtained in this study, therefore, must be considered in conjunction with other information in evaluating the effect of gravity on the outcome of the Lal/Kroes experiment. The results of this study indicate gravity induced convection velocities ranging from approximately 2×10^{-5} to 2×10^{-3} cm/sec for typical orbital gravity loads of 10^{-6} to 10^{-4} g_e. Although these velocities appear to be extremely small, they are comparable to the expected crystal growth rate velocities and molecular diffusion velocities.

REFERENCES

1. Lal, R. B., and R. E. Kroes, "Experiment Requirements and Implementation Plan for Experiment MPS 770058: Solution Growth of Crystals in Zero-G," National Aeronautics and Space Administration, George C. Marshall Space Flight Center, Huntsville, Ala., August 1980.

2. Spradley, Lawrence, and M. L. Pearson, "GIM Code User's Manual for the STAR-100 Computer," NASA Contractor Report 3157, November 1979.

Part 2

NUMERICAL SIMULATION OF NATURAL CONVECTION WITH GRAVITY-SHIFT IN CIRCULAR CYLINDERS IN LOW GRAVITY

ABSTRACT

A numerical analysis was performed to simulate natural convection in circular cylinder enclosures with gravity shifts similar to what might be expected on board an orbiting spacecraft. The particular cases investigated were for a vertical Rayleigh number (based on the vertical component of gravity) of 1000 with superimposed horizontal Rayleigh numbers of ±1000 to ± 000. The initial temperature gradient was taken to be in the direction of the horizontal. For a given set of vertical and horizontal gravity components, the results at steady state were found to be the same regardless of the order in which the two components were imposed. A supercritical horizontal Rayleigh number case with no vertical component was simulated to investigate transient development of convective flow from rest. The convective flow was found to grow exponentially from a small perturbation until steady state is approached. The numerical results for both subcritical and supercritical Rayleigh numbers were found to agree closely with results predicted by a simple analytical model derived for simultaneous loading of both vertical and horizontal components.

CONTENTS

FOREWORD	ii
ABSTRACT	iii
ACKNOWLEDGMENT	iv
NOMENCLATURE	vi
INTRODUCTION	1
PROBLEM FORMULATION AND NUMERICAL SIMULATION	2
RESULTS	4
APPENDIX: Simplified Analytical Model for Natural Convection in a Horizontal Two-Dimensional Circular Enclosure	A-1

NOMENCLATURE

Symbol	Description
d	cylinder diameter = 2 R
g	gravity force
g_H	horizontal g component
g_V	vertical g component
r	radial distance
R	cylinder radius
Ra	Rayleigh number = $\frac{g\beta \Delta T d^3}{\nu\alpha}$
Ra_H	horizontal Rayleigh number
Ra_V	vertical Rayleigh number
T	temperature
T_o	initial mid-point temperature
ΔT	temperature difference across circular cylinder
t	time
$\tilde{t}$	dimensionless time = $\nu t/R^2$
v	velocity
v_{max}	spatial maximum velocity
v_{max_o}	v_{max} for zero horizontal gravity component
Δv_{max}	$v_{max} - v_{max_o}$
$\tilde{v}$	dimensionless velocity = $\frac{128\nu}{g\beta \Delta T d^2}$ v
x, y	rectangular coordinates (Fig. 1)
α	thermal diffusivity
β	volumetric coefficient of thermal expansion

NOMENCLATURE (Concluded)

Symbol	Description
θ	polar angle (Fig. 1)
μ	dynamic viscosity
ν	kinematic viscosity, μ/ρ
ψ	stream function
ρ	density
ρ_o	ρ at $T = T_o$

INTRODUCTION

Some of the fluid mechanics experiments planned to be performed aboard the forthcoming Space Shuttle/Spacelab flights are intended to investigate the use of the near-zero gravity conditions in orbit for various materials processing applications. The near elimination of gravity-induced convective stirring under orbital conditions is expected to yield various high quality specialized products that cannot easily be produced under terrestrial gravity conditions

A number of theoretical and experimental studies have been made of convective flows within various geometric enclosures. Batchelor (Ref. 1) and Weinbaum (Ref. 2) investigated, respectively, rectangular and circular two-dimensional enclosures using non-numerical analytical methods for steady state conditions. Dressler (Ref. 3) recently extended Weinbaum's steady state results for the cylinder to include a transient solution. These analytical results are valid only for low Rayleigh numbers. Robertson and Spradley (Ref. 4) performed numerical analyses to show that the low Rayleigh number analytical theory is valid for Rayleigh numbers up to approximately 1000. All of these investigations have assumed terrestrial-like constant gravity conditions.

In the near-zero gravity environment aboard orbiting spacecraft, the small accelerations that simulate residual gravity conditions are likely to change with time in both magnitude and direction. The purpose of this numerical study is to predict convective flows in circular enclosures with gravitational loads that do not remain fixed in time. The Lockheed-developed General Interpolant Method (GIM) computer code (Ref. 5) was used in the numerical computations. The computations were performed on the NASA-Langley Cyber 203 system.

PROBLEM FORMULATION AND NUMERICAL SIMULATION

The problem investigated is that of two-dimensional natural convection within the circular cylinder enclosure shown in Fig. 1.

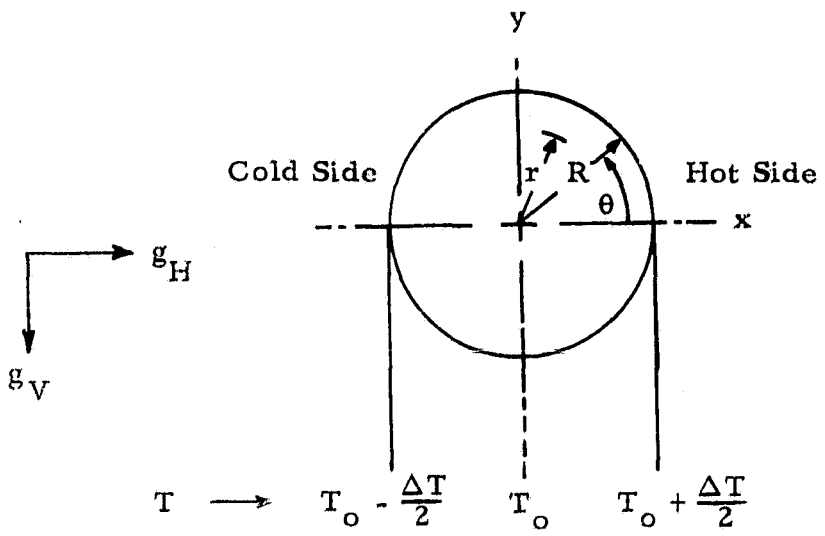

Fig. 1 - Geometry for Circular Cylinder Enclosure

The initial temperature distribution was based on a linear horizontal gradient in the positive x direction, with the boundary points held constant in time:

$$T(r,o) = T_o + (\Delta T/2)\, x/R$$

$$T(R,t) = T_o + (\Delta T/2)\cos\theta \qquad (1)$$

The gravitation loading consisted of two components, a vertical component g_V in the negative y direction and a horizontal component in either the positive or negative x direction. We investigated applying the gravitational components in the following sequences: (1) the vertical component applied until steady state, followed by the horizontal component superimposed to produce a new

steady state; (2) both components applied simultaneously until steady state; and (3) the horizontal component applied first followed by the vertical component.

The numerical simulation was based on a nodal point distribution generated by the GIM code geometry module by specifying an array of 20 x 20 area elements with 21 x 21 nodal points. The circle was treated as a four-sided figure, each side being a quarter-circle arc. Using stretching functions, the circular area was divided into generalized quadrilateral elements with curvilinear sides, with the nodal points located at the four corners of each element. The circular geometry is shown in Fig. 2 with the computational grid network superimposed.

For convenience in the numerical simulation, we assumed a cylinder radius R of 1 cm and a temperature difference ΔT of 100 C. The gravity components were changed accordingly to yield the proper Rayleigh number values. The fluid was assumed to have the thermophysical properties of water and to behave as a Boussinesq fluid in its thermal expansion characteristics. The thermophysical properties used in the numerical simulation are listed as follows:

Property	Value
Viscosity, μ	1 centipoise
Thermal conductivity, k	0.00143 cal/cm-sec-C
Density, ρ	1 gm/cu cm
Specific heat, C_p	1 cal/gm-C
Thermal expansion coefficient, β	2.07×10^{-4}/C

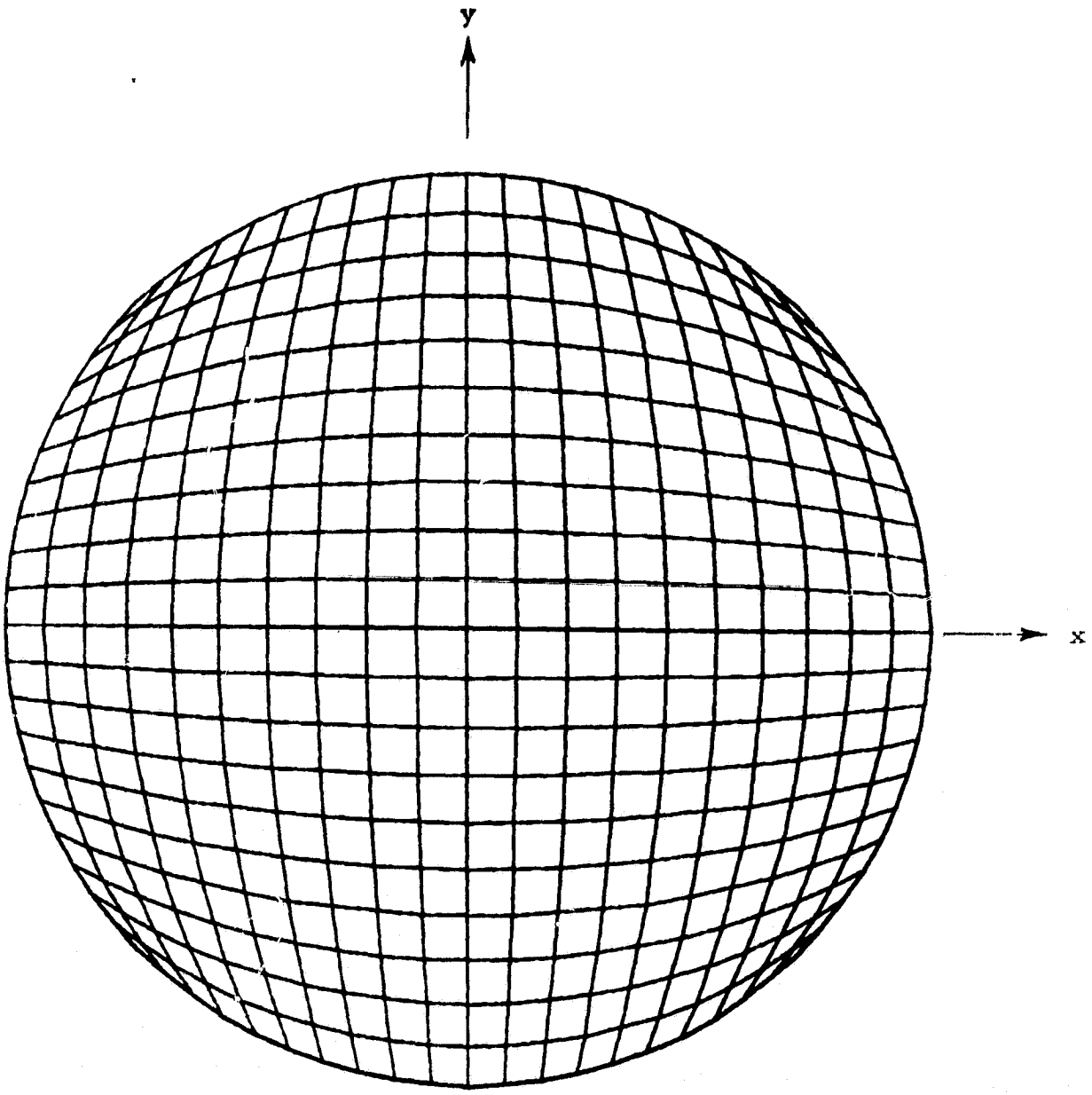

Fig. 2 - Geometry and Computational Grid for Numerical Simulation

RESULTS

Results were obtained for a vertical Rayleigh number, Ra_V, of 1000 and and horizontal Rayleigh numbers, Ra_H, of $\pm$1000, $\pm$2000, and $\pm$5000. We found that the final steady state result for a given set of vertical and horizontal gravity components is the same regardless of the order in which the two components are applied. The steady state spatial maximum velocities for the various Rayleigh number combinations are presented in Fig. 3 in terms of a percentage deviation from the $Ra_H = 0$ case. These results are compared to a simplified analytical theory derived in the appendix for the case of simultaneous impulse applications of the vertical and horizontal gravity components. Reasonable agreement with the analytical prediction is shown in this comparison, particularly for low horizontal Rayleigh numbers. The numerical results show an increase in the spatial maximum of about 150% for a positive horizontal Rayleigh number of 5000 and a decrease of about 40% for a negative Rayleigh number of 5000. Note that the percent deviation depends only on the magnitude of the horizontal Rayleigh number.

The simplified analytical theory, in agreement with Weinbaum (Ref. 2), predicts that, for a zero vertical Rayleigh number, convective flow will not develop for horizontal Rayleigh numbers less than 9216. The GIM code, however, probably due to numerical noise in the program, will generate a small convective flow at subcritical Rayleigh numbers. Superimposing a vertical gravity component on these results leads to a duplication of the results obtained by applying the gravity components either in the reverse order or simultaneously.

The temperature contours at steady state are presented in Fig. 4 for a vertical Rayleigh number of 1000 and horizontal Rayleigh numbers of 0, +1000 and $\pm$5000. The positive horizontal components are shown to noticeably

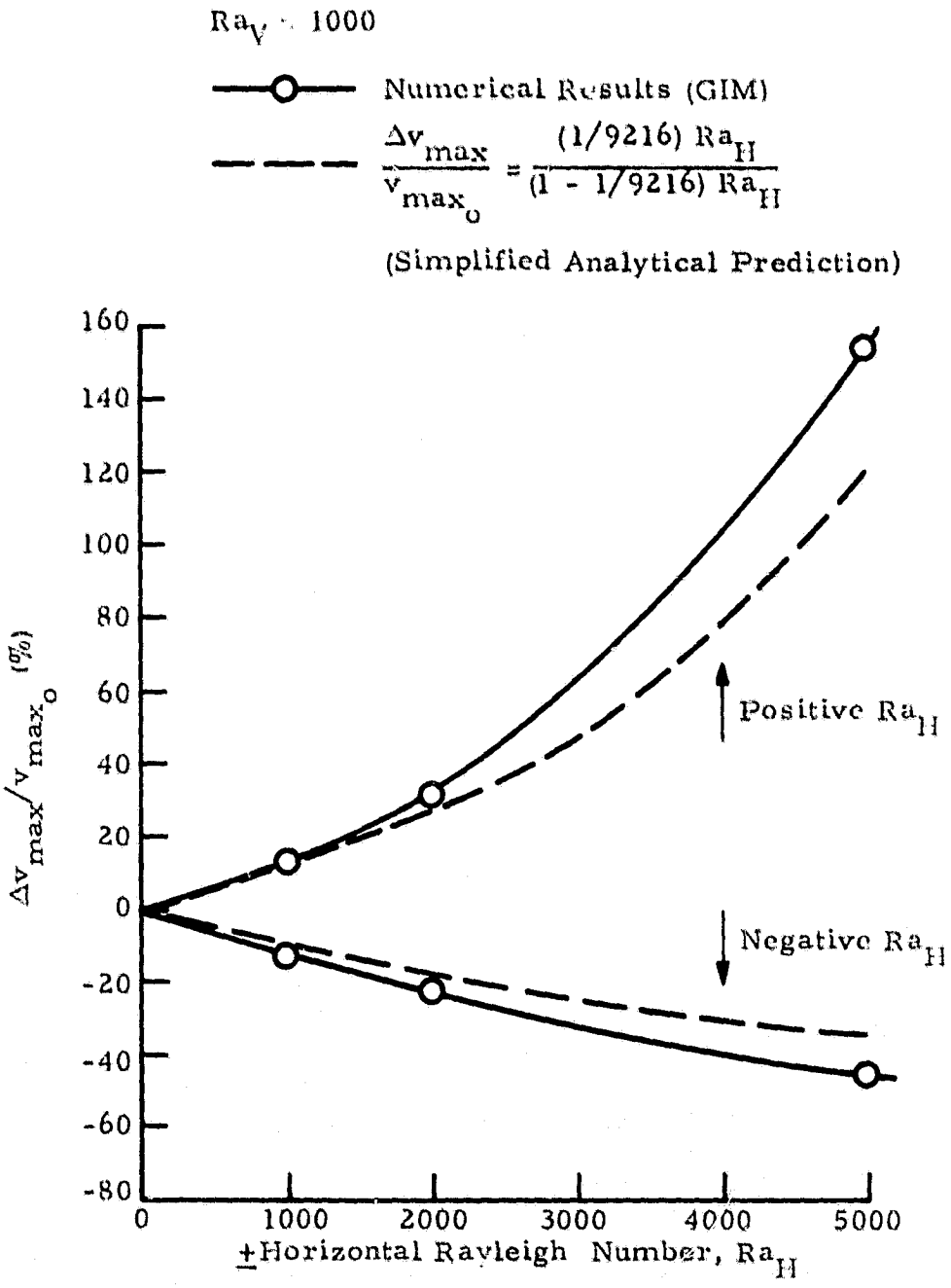

Fig. 3 - Percent Change in Spatial Maximum Velocity vs Horizontal Rayleigh Number

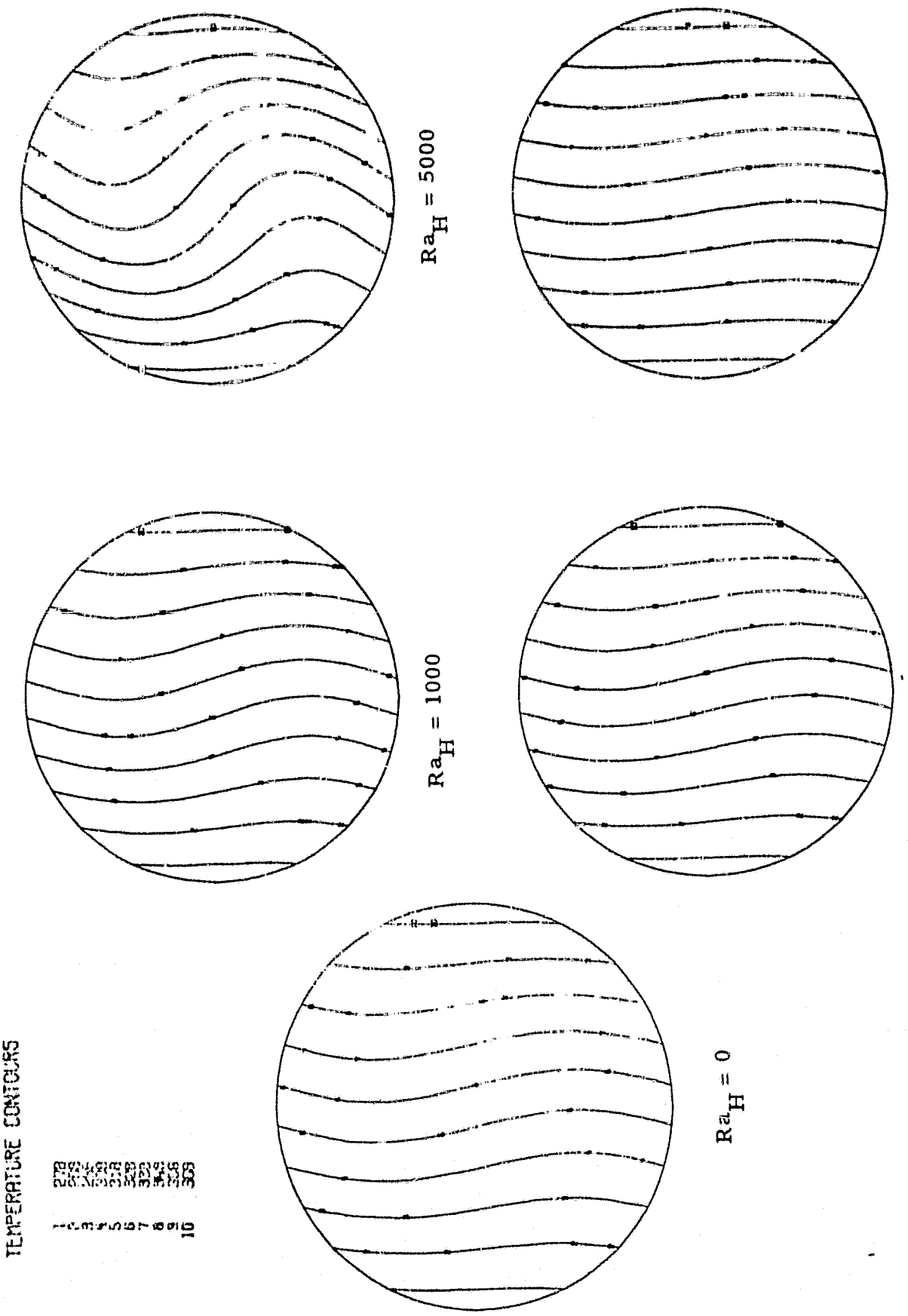

Fig. 4 - Temperature Contours at Steady State for Various Horizontal Rayleigh Numbers (Ra_V = 1000, Temperature Units = K)

increase the distortion in the isotherms as expected. The negative horizontal components decrease the distortion somewhat, but not as noticeably as in the positive cases.

The velocity contours at steady state are shown in Fig. 5, again for a vertical Rayleigh number of 1000 and horizontal Rayleigh numbers of 0, $\pm$1000 and $\pm$5000. The exhibited flow appears to be nearly perfectly circular in all cases, with the maximum velocity indicated roughly near the r = 0.5 to 0.6 radial position. The theoretical maximum occurs at $r = 1/\sqrt{3} = 0.58$ (see Appendix). Some of the departure from circular symmetry in the velocity contours is probably due to the numerical noise in computing such small velocities. The circularity of the flow is more clearly indicated by the steamline contours shown in Fig. 6. A nearly perfectly circular flow pattern is shown in all cases.

A supercritical horizontal Rayleigh number case was simulated to investigate the transient development of convective flow from rest. The Ra_H = 10,000 case was selected with no vertical component. A small initial velocity perturbation in the flow field is required to start the development of convective flow. According to the simplified theory outlined in the Appendix, this velocity perturbation should grow exponentially until the simplified theory is no longer applicable. We started the numerical simulation with a velocity perturbation of 10^{-10} cm/sec in a counterclockwise direction. The resulting flow development is shown in the plot of spatial maximum velocity as a function of time in Fig. 7. In the first stage of the numerical simulation, the computed velocities rapidly increased to levels beyond that expected from the simplified theory, then decreased to a lower level. At this point the flow began to rise exponentially approximately as predicted by the simplified theory. The first stage of the numerical simulation probably represents a numerical noise. After this period of adjustment, the simulated flow development takes on an apparently realistic trend. Note that the initial slope in the nearly linear portion of the logarithmic plot is 0.64 compared to 0.89 predicted by the simplified theory for a Rayleigh number of 10,000. The flow peaks out and reaches a steady state dimensionless spatial maximum

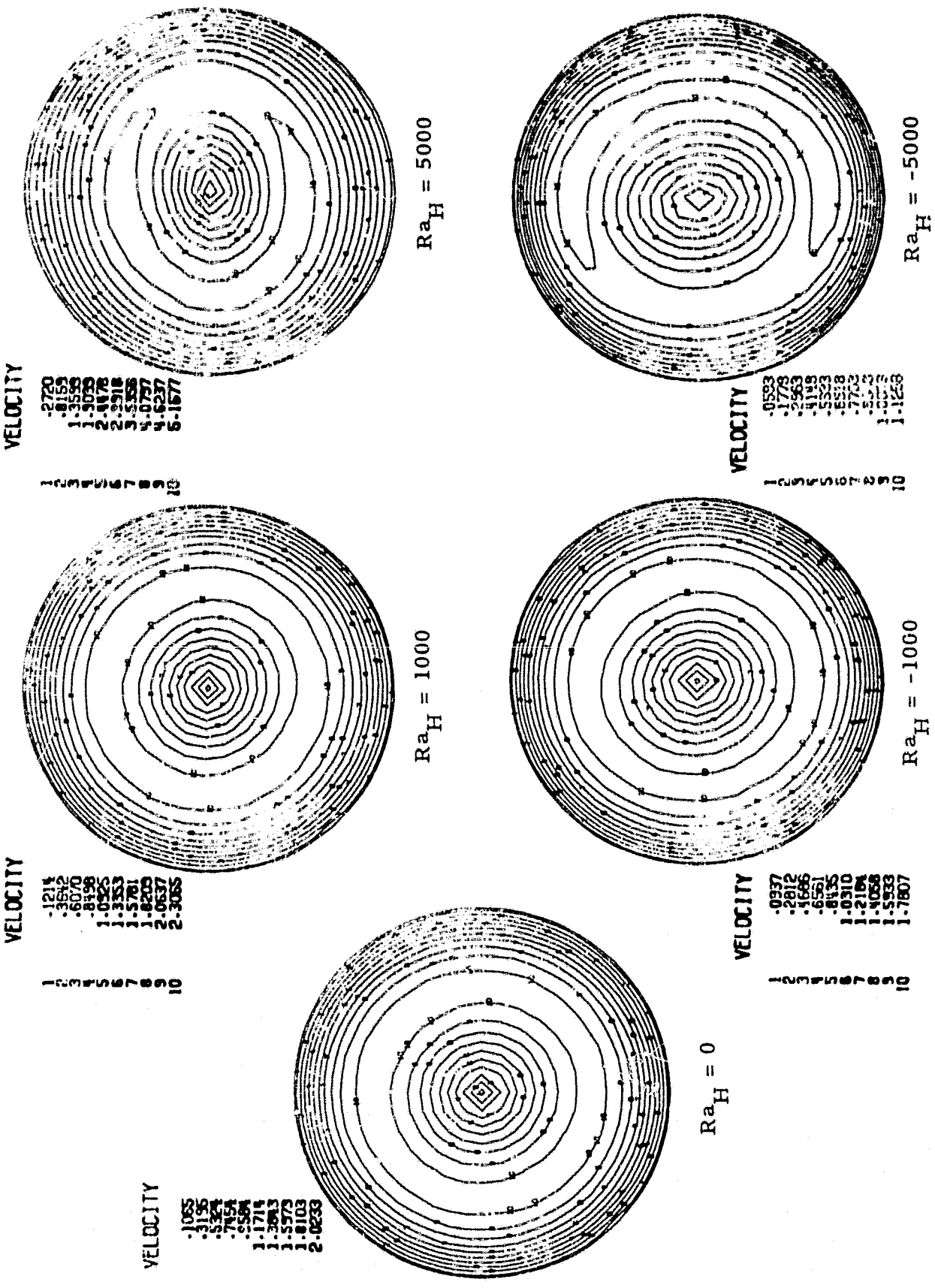

Fig. 5 - Velocity Contours at Steady State for Various Horizontal Rayleigh Numbers (Ra_V = 1000, Velocity Units = 10^{-3} cm/sec).

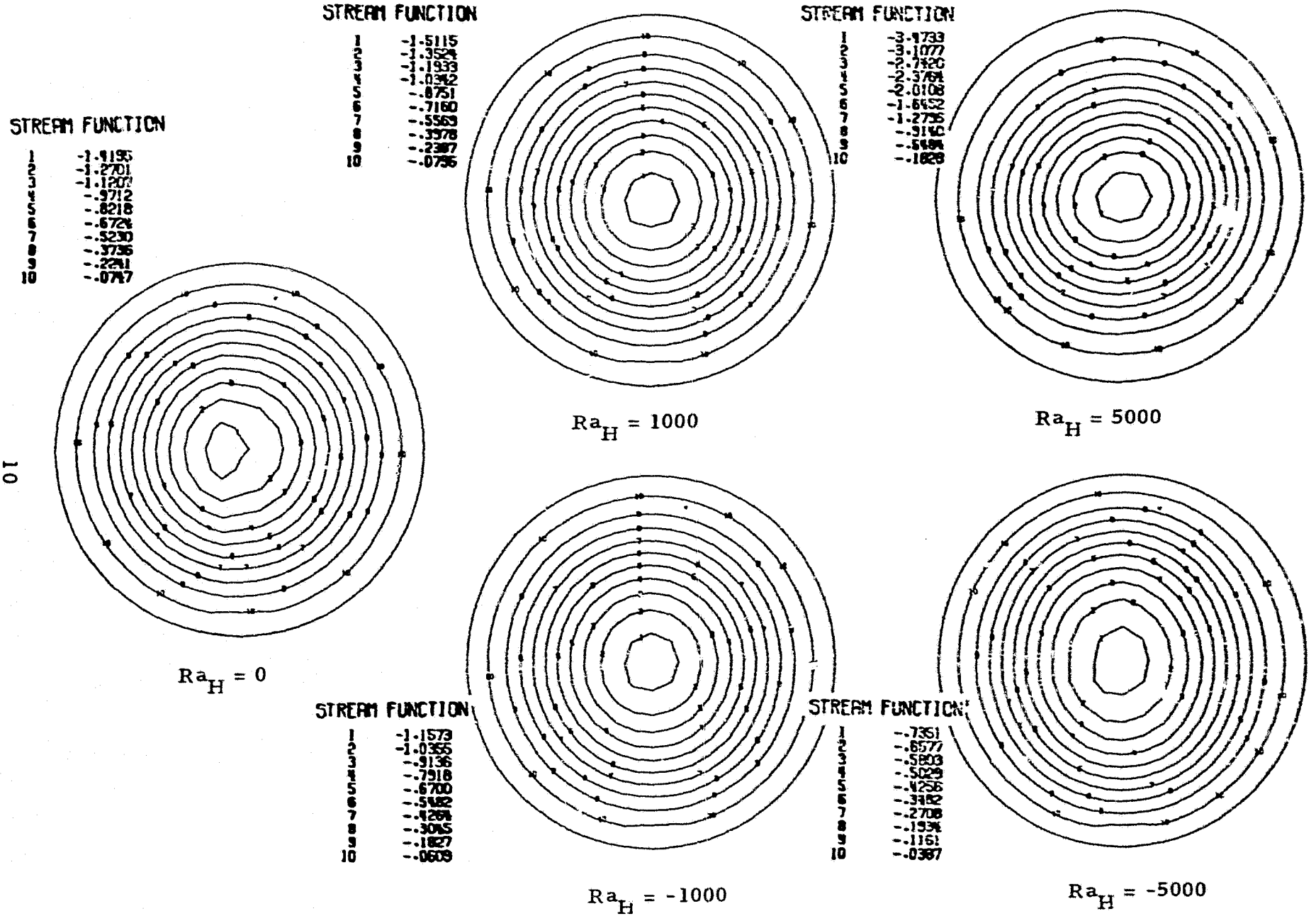

Fig. 6 - Streamlines at Steady State for Various Horizontal Rayleigh Numbers

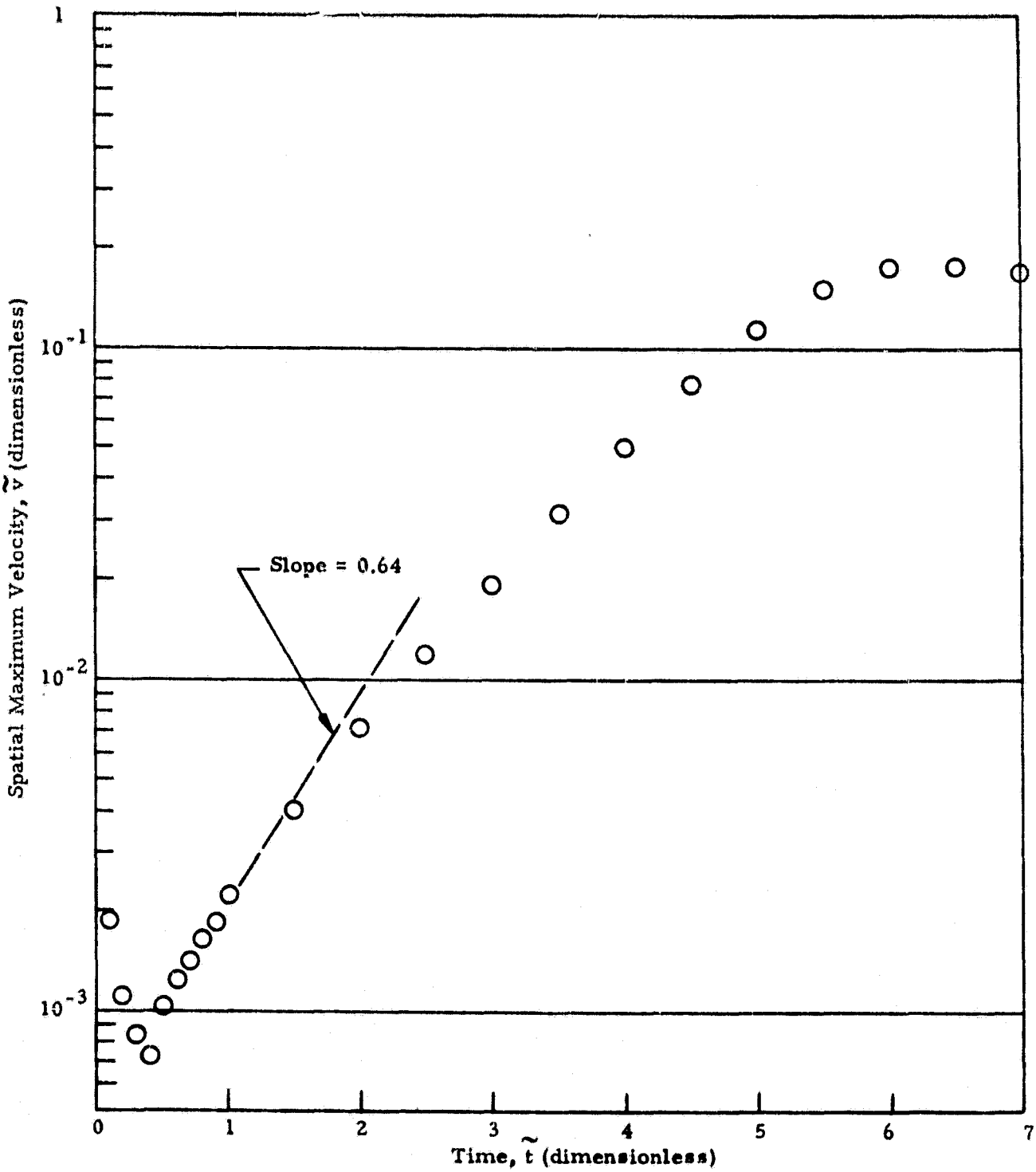

Fig. 7 - Spatial Maximum Velocity as a Function of Time for Supercritical Horizontal Rayleigh Number

velocity of approximately 0.2 after a dimensionless time of approximately 6. This steady state velocity is of the same order as the 0.385 dimensionless velocity (Ref. 4) corresponding to a purely vertical gravity component. Theoretically, the time required to reach steady state depends on the magnitude of the initial velocity perturbation, which is arbitrary. Our computed time to reach steady state, therefore, is not necessarily representative of actual supercritical cases involving the development of convective flow from rest.

The development of convective flow from rest for the supercritical Ra_H = 10,000 case is illustrated by the contour plots of temperature and streamlines in Fig. 8. Steady state was reached in this case without breakup into multiple convective cells.

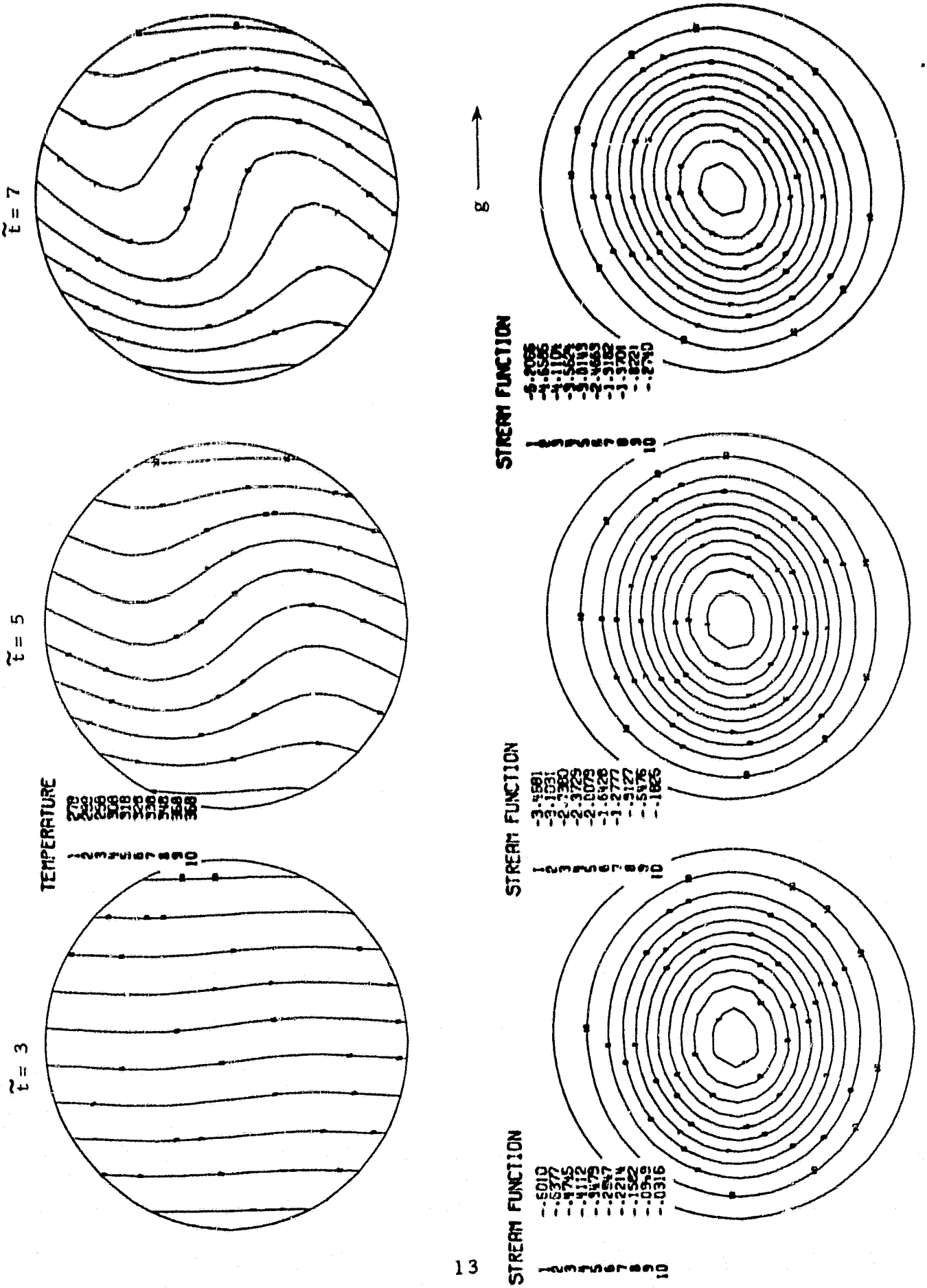

Fig. 8 - Temperature Contours and Streamlines at Various Times for $Ra_H = 10\,000$ ($Ra_V = 0$, Temperature Units = K, Stream Function Units = 10^{-3} cm^2/sec)

CONCLUSIONS

For subcritical horizontal Rayleigh numbers, the imposition of a given set of vertical and horizontal gravity components yields the same steady state convective flow field regardless of the order in which the two components are imposed. For supercritical horizontal Rayleigh numbers without a vertical component, the convective velocity initially grows exponentially from a small perturbation until steady state conditions are approached. For both subcritical and supercritical Rayleigh numbers, the computer simulation results agree reasonably well with predictions based on a simple analytical model.

REFERENCES

1. Batchelor, C.W., "Heat Transfer by Free Convection Across a Closed Cavity Between Vertical Boundaries at Different Temperatures," Quart. Appl. Math., Vol.12, No.3, 1954, p.209.

2. Weinbaum, S., "Natural Convection in a Horizontal Circular Cylinder," J. Fluid Mech., Vol.18, 1964, p.409.

3. Dressler, R.F., NASA Headquarters, Washington, D.C. (to be published).

4. Robertson, S.J., L.W. Spradley, and M.P. Goldstein, "Numerical Analysis of Natural Convection in Two-Dimensional Square and Circular Containers in Low Gravity," LMSC-HREC TR D697821, Lockheed Missiles & Space Company, Inc., Huntsville, Ala., August 1980.

Appendix

SIMPLIFIED ANALYTICAL MODEL FOR NATURAL CONVECTION IN A HORIZONTAL TWO-DIMENSIONAL CIRCULAR ENCLOSURE

Appendix

All previous analyses, including Weinbaum (Ref. 2), Dressler (Ref. 3) and Robertson and Spradley (Ref. 4) have demonstrated that the steady state flow pattern is circular with the velocity given by

$$v = \frac{3\sqrt{3}}{2} \; v_{max} \left[1 - (r/R)^2\right](r/R) \tag{A.1}$$

For simplicity, we assume that the transient flow maintains the same form as Eq. (A.1) with v_{max} varying with time.

Based on the shape of the temperature isotherms noted in Ref. 2, we assume that the temperature distribution is given by

$$T = T_o + \frac{\Delta T}{2} (r/R) \cos\theta + T' \tag{A.2}$$

where T' is a perturbation term due to convective flow given by

$$\begin{aligned} T' &= A \left[1 - (r/R)^2\right] (r/R) \sin\theta \\ &= A \left[1 - (x^2 + y^2)/R^2\right](y/R) \end{aligned} \tag{A.3}$$

Along the y axis ($\theta = \pi/2$), the perturbed temperature distribution defined by Eq. (A.3) follows the same form as the velocity distribution given by Eq. (A.1).

We determined the constant, A, in Eq. (A.3) by satisfying the steady state conduction equation shown below.

$$\vec{v} \cdot \nabla T = \alpha \nabla^2 T \tag{A.4}$$

at the point of maximum velocity and temperature perturbation along the y axis, $r = 1/\sqrt{3}$ ($x = 0$, $y = 1/\sqrt{3}$). A more accurate method of accomplishing this perhaps, would be by minimizing error in Eq. (A.4) over the entire circular region, rather than concentrating on the maximum velocity and temperature perturbation point. For the simplified solution that we are seeking, however, the approach we selected seems appropriate. Finding the temperature gradient and Laplacian at $x = 0$ and $y = 1/\sqrt{2}$ from Eqs. (A.2) and (A.3) and solving Eq. (A.4) yields:

$$A = \frac{\sqrt{3}}{16} \frac{v_{max} R \Delta T}{\alpha} \tag{A.5}$$

The torque, M_V, on the fluid mass due to viscous shear stress on the interior cylinder surface is given by

$$M_V = 2\pi R\mu \left.\frac{\partial v}{\partial r}\right|_{r=R}$$

$$= -6\pi \sqrt{3}\, \mu v_{max} R \tag{A.6}$$

We take the counter-clockwise direction as positive, since the convective flow will assume this direction.

The fluid density distribution is based on a Boussinesq variation with temperature:

$$\rho = \rho_o \left[1 - \beta (T - T_o)\right] \tag{A.7}$$

which, from Eq. (A.2), becomes:

$$\rho = \rho_o \left\{1 - \beta \left[\frac{\Delta T}{2} (r/R) \cos\theta + T'\right]\right\} \tag{A.8}$$

The torque due to gravity M_G is found by:

$$M_G = - \iint \rho (g_V x + g_H y) \, dS \tag{A.9}$$

where the integration is carried out over the circular region. The vertical gravity component g_V is always positive and acts in the negative y direction. The horizontal component, g_H, may be either positive or negative according to its direction with respect to the x axis. Carrying out the integration of Eq. (A.9) yields

$$M_G = - \int_o^{2\pi} \int_o^R \rho (g_V \cos\theta + g_H \sin\theta) \, r^2 \, dr \, d\theta$$

$$= \frac{\pi}{8} \rho_o \beta \Delta T \, R^3 \left(g_V + \frac{\sqrt{3} \, v_{max} \, R}{24 \alpha} g_H\right) \tag{A.10}$$

The instantaneous angular momentum of the fluid mass is given by:

$$P = \iint r \rho v \, dS \tag{A.11}$$

where, again, the integration is carried out over the circular region. Carrying out this integration yields

$$P = \int_0^{2\pi} \int_0^{R} \rho v r^2 \, dr \, d\theta$$

$$= \frac{\sqrt{3}}{4} \pi R^3 \rho_o v_{max} \tag{A.12}$$

By balancing the rate of change of angular momentum to the net torque on the fluid mass, a differential equation is obtained for the variation of v_{max} with time:

$$dP/dt = M_G + M_V$$

$$\frac{\sqrt{3}}{4} \pi R^3 \rho_o \dot{v}_{max} = \frac{\pi}{8} \rho_o \beta \Delta T R^3 \left(g_V + \frac{\sqrt{3} R g_H}{24\alpha} v_{max} \right) - 6\pi \sqrt{3} \mu R v_{max} \tag{A.13}$$

Re-arranging Eq. (A.13) yields:

$$\dot{v}_{max} = \frac{1}{16\sqrt{3}} \frac{\alpha \nu}{R^3} Ra_V - 24 \frac{\nu}{R^2} \left(1 - \frac{Ra_H}{9216} \right) v_{max} \tag{A.14}$$

which yields the solution

$$v_{max} = (v_{max})_{t=0} \exp \left[-24 \left(1 - \frac{Ra_H}{9216} \right) \frac{\nu t}{R^2} \right]$$

$$+ \frac{(\alpha/R) Ra_V}{384\sqrt{3} \left(1 - \frac{Ra_H}{9216} \right)} \left\{ 1 - \exp \left[-24 \left(1 - \frac{Ra_H}{9216} \right) \frac{\nu t}{R^2} \right] \right\} \tag{A.15}$$

where $(v_{max})_{t=0}$ is an initial small perturbation in v_{max}. Note that for zero vertical gravity component ($Ra_V = 0$), any initial small perturbation in v_{max} will be damped for $Ra_H < 9216$. The value 9216, therefore, is the critical Rayleigh number for initiating convective flow for cases where the gravitational vector is in the direction of the temperature gradient. This value agrees with Weinbaum's (Ref. 2) stability analysis for the horizontal cylinder (Weinbaum's value of 576 is based on a definition of Rayleigh number which differs by a factor of 16 from our Rayleigh number).

For $Ra_V > 0$ and $Ra_H < 9216$, Eq. (A.15) yields the steady state result:

$$v_{max} = \frac{v_{max_o}}{1 - \frac{Ra_H}{9216}} \tag{A.16}$$

where v_{max_o} is the maximum velocity for a vertical component only ($Ra_H = 0$):

$$v_{max_o} = \frac{1}{384\sqrt{3}} \frac{\alpha}{R} Ra_V \tag{A.17}$$

The fractional deviation in v_{max} due to a side load is given by:

$$\frac{v_{max} - v_{max_o}}{v_{max_o}} = \frac{Ra_H}{1 - \frac{Ra_H}{9216}} \tag{A.18}$$

For horizontal Rayleigh numbers approaching or greater than the critical value of 9216, this simplified analysis is no longer applicable.

Part 3

EFFECT OF CONTAINER SHAPE ON NATURAL CONVECTION IN ENCLOSURES

Numerical computations were made of natural convection in two-dimensional enclosures of various shape but of equal cross sectional area. Results were obtained for enclosures with circular, half-circular and square shapes. For the shapes investigated, the maximum convective velocity was found to be about the same for all shapes. This suggests that, as a general rule, complicated container shapes can be approximated by simpler shapes of equal area for purposes of predicting the intensity of natural convection in experiment configurations. Additional computations are planned for other enclosure shapes, such as a triangle and rectangle. The complete results will be documented in the future as a Lockheed technical report and as a paper in the open scientific literature.